AMERICAN SOCIETY FOR MICROBIOLOGY | Applied and Environmental Microbiology®

PUBLIC AND ENVIRONMENTAL HEALTH MICROBIOLOGY

1,4,7-Triazacyclononane Restores the Activity of β-Lactam Antibiotics against Metallo-β-Lactamase-Producing *Enterobacteriaceae*: Exploration of Potential Metallo-β-Lactamase Inhibitors

Anou M. Somboro,[a,b] Daniel G. Amoako,[a,b] John Osei Sekyere,[c] Hezekiel M. Kumalo,[d] René Khan,[d] Linda A. Bester,[b] Sabiha Y. Essack[a]

[a]Antimicrobial Research Unit, School of Health Sciences, University of KwaZulu-Natal, Durban, South Africa
[b]Biomedical Resource Unit, College of Health Sciences, University of KwaZulu-Natal, Durban, South Africa
[c]Department of Medical Microbiology, Faculty of Health Sciences, University of Pretoria, Pretoria, South Africa
[d]Discipline of Medical Biochemistry, School of Laboratory Medicine and Medical Science, University of KwaZulu-Natal, Durban, South Africa

ABSTRACT Metallo-β-lactamase (MBL)-producing *Enterobacteriaceae* are of grave clinical concern, particularly as there are no metallo-β-lactamase inhibitors approved for clinical use. The discovery and development of MBL inhibitors to restore the efficacy of available β-lactams are thus imperative. We investigated a zinc-chelating moiety, 1,4,7-triazacyclononane (TACN), for its inhibitory activity against clinical carbapenem-resistant *Enterobacteriaceae*. MICs, minimum bactericidal concentrations (MBCs), the serum effect, fractional inhibitory concentration indexes, and time-kill kinetics were determined using broth microdilution techniques according to Clinical and Laboratory Standards Institute (CSLI) guidelines. Enzyme kinetic parameters and the cytotoxic effects of TACN were determined using spectrophotometric assays. The interactions of the enzyme-TACN complex were investigated by computational studies. Meropenem regained its activity against carbapenemase-producing *Enterobacteriaceae*, with the MIC decreasing from between 8 and 64 mg/liter to 0.03 mg/liter in the presence of TACN. The TACN-meropenem combination showed bactericidal effects with an MBC/MIC ratio of ≤4, and synergistic activity was observed. Human serum effects on the MICs were insignificant, and TACN was found to be noncytotoxic at concentrations above the MIC values. Computational studies predicted that TACN inhibits MBLs by targeting their catalytic active-site pockets. This was supported by its inhibition constant (K_i), which was 0.044 μM, and its inactivation constant (K_{inact}), which was 0.0406 min^{-1}, demonstrating that TACN inhibits MBLs efficiently and holds promise as a potential inhibitor.

IMPORTANCE Carbapenem-resistant *Enterobacteriaceae* (CRE)-mediated infections remain a significant public health concern and have been reported to be critical in the World Health Organization's priority pathogens list for the research and development of new antibiotics. CRE produce enzymes, such as metallo-β-lactamases (MBLs), which inactivate β-lactam antibiotics. Combination therapies involving a β-lactam antibiotic and a β-lactamase inhibitor remain a major treatment option for infections caused by β-lactamase-producing organisms. Currently, no MBL inhibitor–β-lactam combination therapy is clinically available for MBL-positive bacterial infections. Hence, developing efficient molecules capable of inhibiting these enzymes could be a promising way to overcome this phenomenon. TACN played a significant role in the inhibitory activity of the tested molecules against CREs by potentiating the activity of carbapenem. This study demonstrates that TACN inhibits MBLs efficiently and holds promises as a potential MBL inhibitor to help curb the global health threat posed by MBL-producing CREs.

Citation Somboro AM, Amoako DG, Osei Sekyere J, Kumalo HM, Khan R, Bester LA, Essack SY. 2019. 1,4,7-Triazacyclononane restores the activity of β-lactam antibiotics against metallo-β-lactamase-producing *Enterobacteriaceae*: exploration of potential metallo-β-lactamase inhibitors. Appl Environ Microbiol 85:e02077-18. https://doi.org/10.1128/AEM.02077-18.

Editor Hideaki Nojiri, University of Tokyo

Address correspondence to Anou M. Somboro, anou.somboro@gmail.com.

Received 25 August 2018
Accepted 24 October 2018
Accepted manuscript posted online 26 November 2018
Published 23 January 2019

KEYWORDS *Enterobacteriaceae*, metallo-β-lactamase inhibitor, TACN, β-lactams, binding affinity

The broad-spectrum antibiotics known as β-lactams have relatively minimal toxicity, making them the antibiotics of choice for the treatment of many bacterial infections (1). However, the surge in resistance to β-lactams in Gram-negative bacteria is affecting the management of infections worldwide (2). β-Lactams are rendered ineffective through different mechanisms, including reduced membrane permeability through porin downregulation and efflux, target site modification, and, most importantly, the production of β-lactamases, enzymes that hydrolyze β-lactams (3, 4).

Metallo-β-lactamases (MBLs) are Ambler class B β-lactamases with zinc ions at their active sites. The zinc ions orient a hydroxide nucleophile to attack the carbonyl on a β-lactam ring (5, 6). Subclass B1 MBLs are the most clinically relevant among the class B MBLs. They possess a binuclear active site which contains either one or two Zn(II) ions and hydrolyze all β-lactam antibiotics in clinical use except monobactams (7). MBLs, such as New Delhi metallo-β-lactamase (NDM), Verona integron-borne metallo-β-lactamase (VIM), and imipenemase (IMP), mediate high-level resistance to antibiotics in carbapenem-resistant *Enterobacteriaceae* (CRE) (8). CRE have been identified across the globe, including in all African regions (9–11), and have been ranked as critical in the World Health Organization's priority pathogens list for the research and development of new antibiotics (12). It is therefore imperative to invest in the discovery and development of MBL inhibitors (MBLIs) for combination therapy with carbapenems.

Potential MBLIs investigated to date have shown substantial *in vitro* activity but cannot be used clinically due to the simultaneous inhibition of human metalloenzymes or their cytotoxic effects (13–15). MBLIs, such as aspergillomarasmine A (AMA) (14), Ca-EDTA (13), 1,4,7-triazacyclononane-1,4,7-triacetic acid (NOTA), and 1,4,7,10-tetraazacyclododecane-1,4,7,10-tetraacetic acid (DOTA) (16), are the few nontoxic MBLIs identified to date and act by chelating the zinc ions (17).

Herein, we investigated the inhibitory activity of 1,4,7-triazacyclononane (TACN) against well-characterized subclass B1 MBL-producing *Enterobacteriaceae*. TACN has a chemical structure different from that of the other members of the family of metal chelator series that have been reported and has the lowest molecular weight among the members of that family. We believe that exploring and understanding the mechanisms of biologically relevant chemical moieties are the surest ways to find clinically potent MBL inhibitors that will give a lasting solution to this global menace.

(This article was submitted to an online preprint archive [18].)

RESULTS

MICs, MBCs, and the MBC/MIC ratio. TACN is a cyclic organic compound within the NOTA and DOTA series and is derived from cyclononane by the replacement of three equidistant CH_2 groups with NH groups (19) (Fig. 1). It can be seen from the structures that TACN is different from NOTA and DOTA (all of which are in the same family of compounds) (Fig. 1). The results revealed that this molecule (TACN) successfully restored the activity of meropenem (MEM) against characterized clinical isolates of carbapenem-resistant *Enterobacteriaceae* expressing acquired subclass B1 metallo-β-carbapenemases and reference strains with MIC values as low as 0.03 mg/liter, as shown in Tables 1 and 2. Also, various inhibitory concentrations of TACN (varying from 2 mg/liter to 64 mg/liter) considerably enhanced the efficacy of MEM against the MBL-producing bacteria. The lowest concentration of TACN at which most of the MEM activity was restored was 8 mg/liter (Tables 1 and 2). Therefore, all subsequent experiments were conducted with a fixed concentration of 8 mg/liter of TACN. None of the tested serine β-lactamase (SBL) types (*Klebsiella pneumoniae* OXA-48 and *Enterobacter cloacae* KPC-2) was affected by TACN, substantiating the substrate spectrum of this compound (Table 1). The minimal bactericidal concentrations (MBCs) of MEM were determined in the presence of TACN at a fixed concentration, and the MBC/MIC ratio

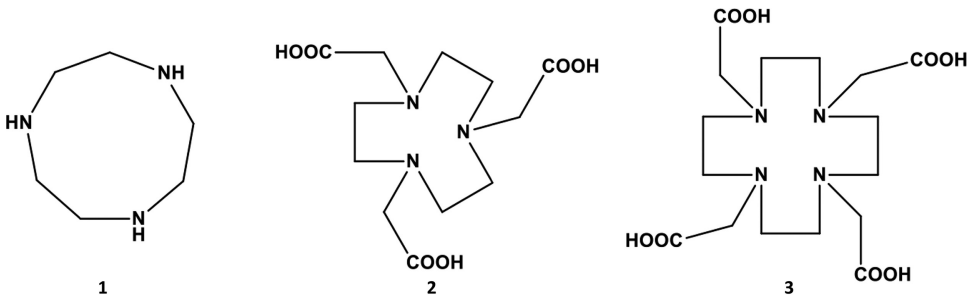

FIG 1 Chemical structures of 1,4,7-triazacyclononane (TACN) (structure 1), 1,4,7-triazacyclononane-1,4,7-triacetic acid (NOTA) (structure 2), and 1,4,7,10-tetraazacyclododecane-1,4,7,10-tetraacetic acid (DOTA) (structure 3).

of the combination ranged from 1- to 4-fold against both the reference and clinical CRE isolates used in this study, except against two clinical isolates, against which 8× the MIC values were required for activity (Table 2). *K. pneumoniae* ATCC BAA 1706 and *Escherichia coli* ATCC 25922 had no changes in their MIC values when challenged with MEM alone and MEM-TACN.

Serum effect on MIC. The MIC values of MEM-TACN combination in the presence of 50% human serum varied from approximately 1- to 4-fold dilutions compared to those of MEM-TACN in the absence of serum, indicating that the inhibition properties of the combination were not affected by the presence of human serum (Table 1).

Synergistic effect of TACN and MEM on CRE reference strains. The synergy between TACN and MEM against CRE isolates was investigated. In most of the cases, the minimum concentrations of TACN alone required to inhibit the MBL-producing *Enterobacteriaceae* were ≥128 mg/liter (Table 1). MEM alone exhibited inhibitory concentrations of ≥8 mg/liter, indicating the carbapenem-resistant phenotype of these pathogens (20). Challenging these CREs with a combined regimen of MEM-TACN potentiated the effectiveness of MEM. The calculated fractional inhibitory concentration (FIC) index of MEM-TACN was ≤0.5, indicating a synergistic effect (Table 1).

Time-kill kinetics. The combination of MEM and TACN caused a considerable decrease in the number of CFU per milliliter relative to the initial bacterial density of approximately 10^6 CFU/ml over time (0, 1, 2, 4, 6, 8, and 24 h) when its activity against the tested isolates at the different multiples of the MIC evaluated in this study (1×, 4×, and 8× the MIC) was tested (Fig. 2). A 10^3-fold decrease in the number of CFU per milliliter was observed at 4 h when the cells were treated with MEM-TACN at 1×, 4×, and 8× the MIC. The time-kill kinetics results indicated that the TACN-MEM combination had bactericidal activity against the selected CRE isolates. When MEM alone at concentrations of 4× and 8× the MIC was used to challenge the isolates, no significant decrease was observed over the time interval of 24 h.

Cytotoxicity. The 3-(4,5-dimethyl-2-thiazolyl)-2,5-diphenyl-2H-tetrazolium bromide (MTT) assay was used to measure TACN cytotoxicity (0 to 1,024 mg/liter) in HepG2 cells after 24 h of exposure. A decrease in cell viability was associated with an increase in the TACN concentration (Fig. 3), and the regression analysis yielded a 50% inhibitory concentration (IC_{50}) of 56 mg/liter. However, this IC_{50} of TACN was far higher than the fixed MIC value of 8 mg/liter used in this study.

Enzymatic assays. TACN efficiently inhibited the activity of NDM-1 in a concentration- and time-dependent manner, as illustrated in Fig. 4A, which shows the effect of increasing concentrations of TACN (0 to 50 μM) on the time-dependent decrease in NDM-1 activity. The kinetic parameters were constructed by nonlinear regression of the observed initial inactivation rate constant (K_{obs})-versus-TACN concentration plot shown in Fig. 4B. TACN possessed an apparent potential inhibition property toward NDM-1 enzymes like aspergillomarasmine A (14), as shown in Fig. 5. The kinetic assay revealed that TACN was a potent time-dependent inhibitor with an inhibition constant (K_i) and an inactivation constant (K_{inact}) of 0.044 ± 0.018 μM and 0.0406 ± 0.007 min^{-1}, respectively.

TABLE 1 Inhibitory activity of TACN and MEM alone and in combination against reference strains of CRE[a]

Enzyme produced and bacterial species	Metallo-β-lactamase produced (class B)	MIC (mg/liter)					MBC (mg/liter) of MEM-TACN8	MBC/MIC ratio of MEM-TACN8	MEM-TACN8 MIC (mg/liter) with serum	FIC index
		MEM alone	TACN alone	{MEM-TACN4}	{MEM-TACN8}	{MEM-TACN16}				
Metallo-β-lactamases										
E. coli	NDM-1	128	1,024	{0.125–4}	{0.125–8}	{0.06–16}	0.5	4	0.25	0.008
E. cloacae	NDM-1	16	>1,024	{0.06–4}	{0.03–8}		0.125	4	0.125	≤0.005
Citrobacter freundii	NDM-1	8	1,024	{0.25–4}	{0.125–8}	{0.125–16}	0.125	1	0.25	0.023
Providencia rettgeri	NDM-1	64	>1,024	{8–4}	{2–8}		2	1	2	≤0.035
Providencia stuartii	NDM-1	16	>1,024	{2–4}	{2–8}		2	1	4	≤0.253
E. coli	NDM-4	128	1,024		{0.125–8}	{0.06–16}	0.125	1	1	0.008
E. coli	VIM-1	32	1,024	{0.25–4}	{0.125–8}	{0.06–16}	0.125	1	0.25	0.011
K. pneumoniae	VIM-1	32	512	{2–4}	{0.125–8}	{0.06–16}	0.5	4	8	0.019
E. cloacae	VIM-1	8	128	{1–4}	{1–8}		1	1	2	0.187
E. coli	VIM-2	8	128	{0.06–4}	{0.03–8}		0.06	2	0.125	0.066
E. cloacae	IMP-1	32	512	{0.25–4}	{0.125–8}		0.5	4	2	0.019
K. pneumoniae	IMP-1	32	512	{8–4}	{4–8}		4	1	16	0.141
E. coli	IMP-1	16	512	{1–4}	{0.06–8}	{0.03–16}	0.125	2	0.25	0.019
E. cloacae	IMP-8	8	512	{0.5–4}	{0.125–8}	{0.03–16}	0.25	2	0.125	0.031
K. pneumoniae	IMP-8	16	1,024	{8–4}	{4–8}	{2–16}	8	2	4	0.250
				{MEM-TACN8}	{MEM-TACN16/32}	{MEM-TACN64}				
Serine-β-lactamases										
K. pneumoniae	OXA-48	8	128	{8–8}	{8–16}	{4–64}	NA	NA	NA	NA
E. cloacae	KPC-2	32	256		{32–32}	{32–64}	NA	NA	NA	NA
ATCC susceptible strains										
K. pneumoniae ATCC BAA 1706	Susceptible strain	0.5	1,024	NE			NA	NA	NA	NA
E. coli ATCC 25922	Susceptible strain	0.03	1,024	NE			NA	NA	NA	NA

[a]TACN4, TACN8, TACN16, TACN32, and TACN64 represent a fixed concentration of 4, 8, 16, 32, and 64 mg/liter TACN, respectively, with various concentrations of meropenem; (in the braces, the first number represents the MIC for MEM and the second number represents the given TACN concentration); NA, not applicable; NE, no inhibitory effect.

TABLE 2 MICs and MBCs of TACN against South African clinical isolates

Bacterial species and isolate	MBL produced (class B)	Other β-lactamase(s) produced	MEM with 8 mg/liter of TACN		
			MIC (mg/liter)	MBC (mg/liter)	MBC/MIC ratio
K. pneumoniae (*n* = 11)					
D(UNN40_S4)	NDM-1	DHA-1, CTX-M-15, SHV-1, OXA-1	0.5	2	4
C(UNN39_S3)	NDM-1	SHV-1, CTX-M-15, OXA-1, DHA-1	0.5	2	4
I(UNN45_S9)	NDM-1	OXA-1, CTX-M-15, SHV-99, TEM-1B	4	8	2
J(UNN46_S10)	NDM-1	OXA-1, CTX-M-15, SHV-1 and -28, DHA-7	0.5	2	4
53_S27	NDM-1	OXA-1, DHA-1, CTX-M-15, SHV-1 and -28	4	16	4
12_S5	NDM-1	CTX-M-15, SHV-1 and -28, DHA-1, OXA-1	2	8	4
13_S6	NDM-1	CTX-M-15, SHV-1 and -28, DHA-7	4	16	4
20_S11	NDM-1	CTX-M-15, TEM-1A, OXA-9, SHV-1 and -28, OXA-1 and -9	0.125	1	4
29_S13	NDM-1	CTX-M-15, SHV-1 and -28, OXA-1 and -9, TEM-1A	0.125	1	4
32_S15	NDM-1	DHA-1, CTX-M-15, SHV-1 and -28, OXA-1	0.125	1	4
21_S12	NDM-1	TEM-1A, SHV-1 and -28, CTX-M-15, OXA1 and -9	0.5	1	2
S. marcescens (*n* = 10)					
B(UNN38_S2)	NDM-1	OXA-10, OXA-1, CTX-M-15, SCO-1, TEM-133, TEM-198	0.125	1	4
E(UNN41_S5)	NDM-1	CTX-M-15, SCO-1, TEM-198, OXA-10, OXA - 1	1	2	2
G(UNN43_S7)	NDM-1	OXA-10, TEM-1B	1	4	4
K(UNN47_S11)	NDM-1	TEM-1B, OXA-1, OXA-10, SCO-1	2	16	8
L(UNN48_S12)	NDM-1	CTX-M-15, OXA-10, OXA -1, SCO-1, TEM-1	2	4	2
7_S3	NDM-1	TEM- 1B, OXA-10	2	8	4
56_S29	NDM-1	None	0.5	2	4
59_S30	NDM-1	TEM-1B, CTX-M-3	1	2	2
67_S33	NDM-1	OXA-10, CTX-M -15, OXA-1, TEM-1, SCO-1	4	16	4
71_S36	NDM-1	CTX-M-11, TEM -1B, OXA -10, OXA-1, SCO-1	2	2	1
E. cloacae (*n* = 9)					
A(UNN37_S1)	NDM-1	CTX-M-3, ACT-3	0.5	1	2
F(UNN42_S6)	NDM-1	CTX-M-15, TEM -1B, OXA-1, ACT-7	0.5	2	4
H(UNN44_S8)	NDM-1	CTX-M-15, TEM -1B, OXA-1, ACT-14	1	1	1
16_S9	NDM-1	CTX-M-15, OXA-1, ACT-4	0.125	2	8
43_S20	NDM-1	TEM -1B, SHV-12, MIR-1	2	4	2
49_S24	NDM-1	CTX-M-15, TEM-1B, OXA-1, ACT-3, CMY-77	0.5	1	2
51	NDM-1	CTX-M-3, TEM-1B, CMY-77	0.25	1	4
55_S28	NDM-1	TEM -1B, ACT-4, SHV-12	4	2	2
63_S31	NDM-1	TEM-1B, ACT-1	0.5	2	4
E. coli 10 (*n* = 1)	NDM-5	CMY-42	2	4	2
C. freundii 48 (*n* = 1)	NDM-1	CTX-M-3, TEM-1B, CMY-77	0.25	2	4
K. oxytoca 69 (*n* = 1)	NDM-1	CTX-M-3, TEM-1B, OXY-14	0.25	2	4

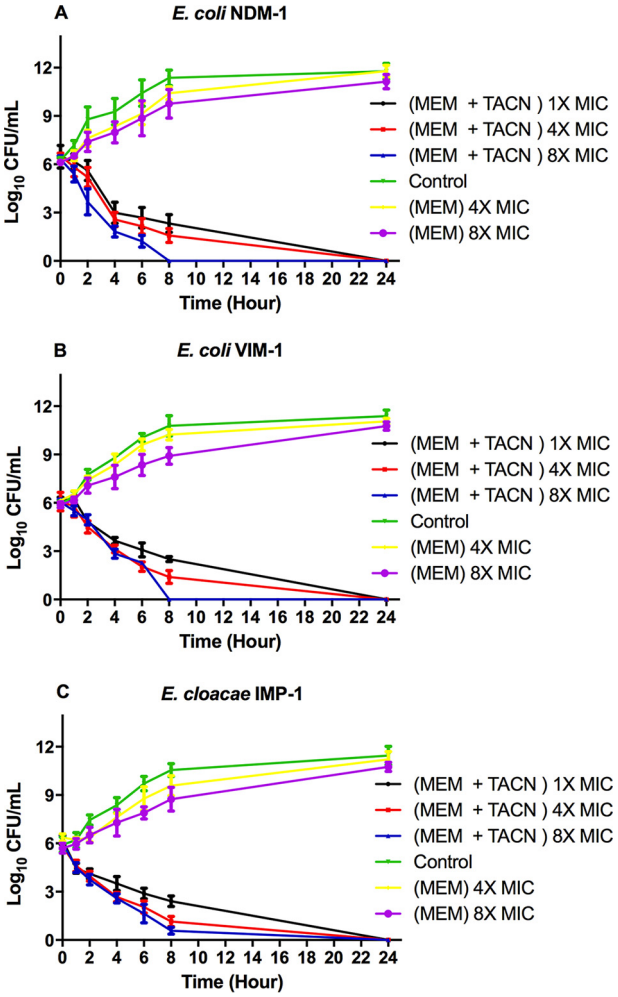

FIG 2 Time-kill kinetics at various concentrations of MEM and a fixed concentration of TACN (8 mg/ml). *E. coli* producing NDM-1 (A), *E. coli* producing VIM-1 (B), and *E. cloacae* producing IMP-1 (C) were challenged with the MEM-TACN combination at 1×, 4×, and 8× the MIC. The surviving CFU were plated at different time intervals (1, 2, 4, 6, 8, 24 h). All data points represent the average results from 3 independent experiments.

Computational simulations. The fluctuations of the enzyme-ligand complex and ligand-associated movements were analyzed to ascertain their structural stability and movements during the simulation. These movements, which ensure their functional reliability and working efficiency, are essential for functionality and existence inside the living system. The overall systems showed appreciable stability, as depicted in Fig. 6.

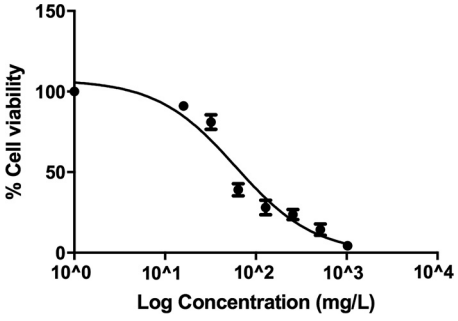

FIG 3 TACN induces a dose-dependent decrease in HepG2 cell viability following treatment for 24 h. Higher TACN concentrations resulted in increased cell death.

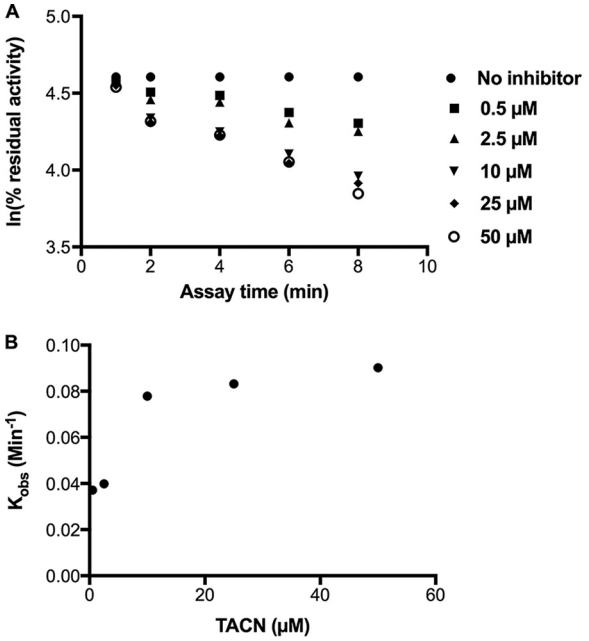

FIG 4 (A) Time- and concentration-dependent inhibition of NDM-1 by TACN. (B) Logarithmic plot of the K_{obs} of TACN against the TACN concentration.

The root mean square deviation (RMSD) of the entire system complex remained stable during the course of simulation of 100 ns.

The calculated binding free energy of TACN to NDM-1 and VIM-2 by the molecular mechanics/Poisson-Boltzmann surface area (MM/GBSA) protocol is shown in Table 3. The calculated contributions favoring the inhibitors' binding included the electrostatic interaction (ΔE_{elec}), which was −9.4229 kcal/mol for the NDM-1_{TACN} complex. The intermolecular van der Waals energy (ΔE_{vdw}) for NDM-1_{TACN} was −46.0898 kcal/mol, which also favored binding. The total binding free energy (ΔG_{bind}) for NDM-1_{TACN} was −39.1603 kcal/mol. A similar trend was also observed in the VIM-2_{TACN} complex, as shown in Table 3. The results suggest that the theoretical calculations of the binding free energies support the experimental findings in terms of the potential of TACN to inhibit the MBL enzymes.

To gain a further understanding of the active-site residue interactions with the compounds, the simulated complexes were observed with LigPlot protein-ligand interaction software. It was observed that the ligand is attached to the active-site residues in all complexes, as shown in Fig. 7. For TACN, the His250 and Asp124 residues provided

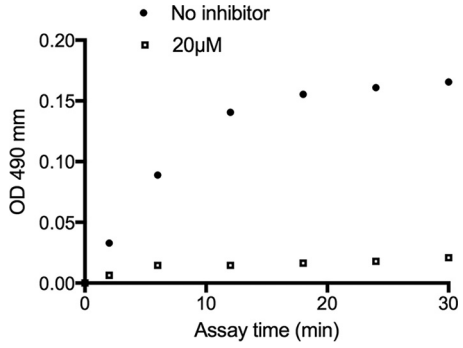

FIG 5 Residual activity after rapid dilution of the enzyme-inhibitor complex. The absorbance changes from the coincubation of NDM-1 with no inhibitor (●) and NDM-1 with TACN (□) are shown. The slope of the initial rate represents the hydrolytic activity of NDM-1. OD, optical density.

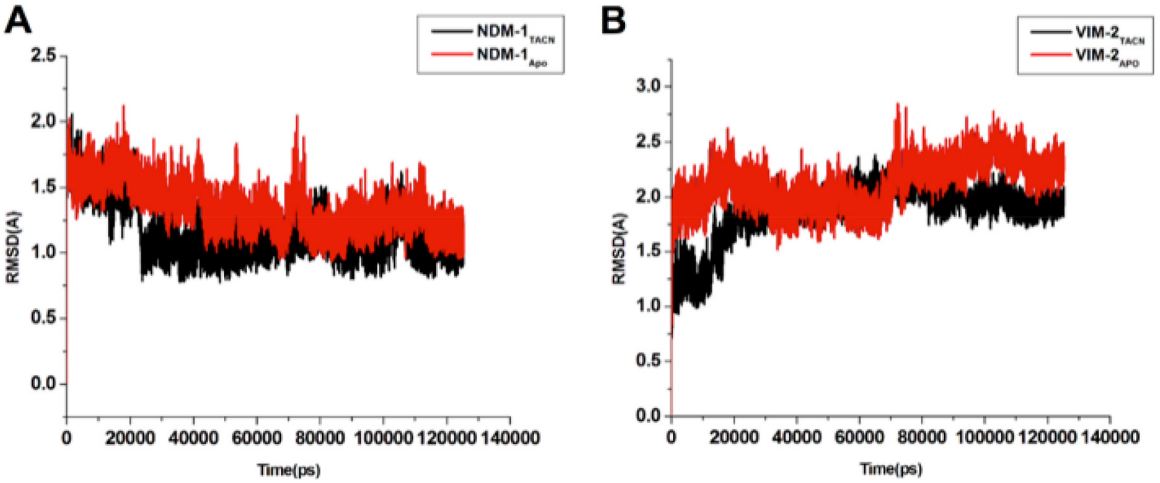

FIG 6 Time-dependent RMSD plots of NDM-1_{TACN} (A) and VIM-2_{TACN} (B). The complexes are represented in black, and the free enzymes are represented in red.

an H-bonding capability, while His122, Asn220, and Trp93 roof the hydrophobic active-site pocket. These residues provide the hydrophobic surface area while maintaining the H-bonding capability.

DISCUSSION

This study evaluated the activity of the TACN-MEM combination against clinical and reference CRE isolates and identified TACN to be a promising MBL inhibitor. The affinity of metal chelators for binding/sequestering metal ions (21), such as zinc at MBLs' active sites, makes them potential inhibitors that can be developed for treating CRE infections. TACN is a metal-chelating agent that exhibited no cytotoxic effect at effective concentrations.

We showed that TACN significantly reduced the MIC of MEM, reinstating the carbapenem's efficacy against 33 South African clinical isolates and 15 MBL-producing reference strains. MEM MICs against all the tested isolates except SBL producers and susceptible ATCC strains decreased by 4- to >512-fold in the presence of TACN. *E. cloacae* and *K. pneumoniae* strains producing the SBLs KPC-2 and OXA-48, respectively, exhibited only 2-fold or no decrease in MEM MICs, showing that the inhibitory effect of TACN was specific for zinc-based β-lactamases. In our previous study, NOTA and DPA [di-(2-picolyl)amine] exhibited similar activity against MBLs at 4 and 8 mg/liter (16, 22). Metal chelators are known for their strong affinity toward metal ions (21). Class B MBLs possess zinc at their active sites, thus enabling TACN to bind or sequester the zinc ions and inhibit the enzymes' β-lactam hydrolysis activity.

MEM regained its pharmacological properties when it was combined with TACN. Most of the tested isolates exhibited an MBC/MIC ratio of $\leq$4, except for two clinical isolates, *Serratia marcescens* and *E. cloacae*, for which the MBC/MIC ratio was 8 (Table 2). Based on the MBC/MIC ratio values, MEM demonstrated its known bactericidal activity in the presence of TACN, and time-kill kinetic studies confirmed the bactericidal property of the MEM-TACN combination. The MEM-TACN combination was synergistic,

TABLE 3 MM/GBSA binding free energy profile for NDM-1_{TACN}, and VIM-2_{TCN}[a]

System	Binding free energy profile (kcal/mol)				
	ΔE_{vdw}	ΔE_{elec}	ΔG_{solv}	ΔG_{gas}	ΔG_{bind}
NDM-1_{TACN} complex	−46.0898	−9.4229	16.3523	−55.5126	−39.1603
VIM-2_{TACN} complex	−50.9300	−9.9143	19.6230	−63.4178	−41.2199

[a]ΔG_{bind}, total binding free energy; ΔE_{elec}, electrostatic interactions; ΔE_{vdw}, intermolecular van der Waals energy; ΔG_{gas}, gas-phase energy; ΔG_{solv}, solvation energy. All binding free energy profiles are rounded to 5 significant figures.

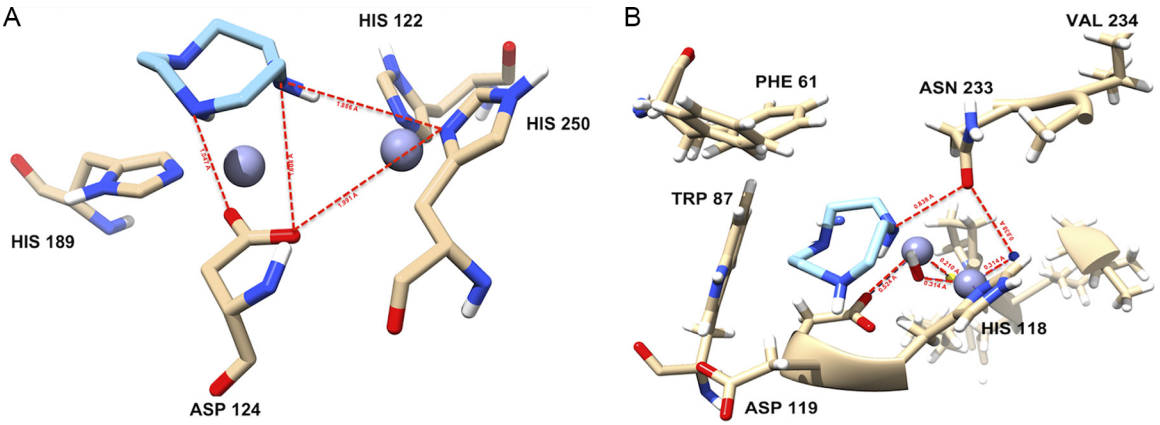

FIG 7 Binding mechanism, illustrated by the interaction of docked ligand (TACN), at the active site of NDM-1 (A) and VIM-2 (B).

with the FIC index ranging from ≤0.005 to 0.25 for all the CRE reference strains used in the study. Aspergillomarasmine A, a metal-chelating agent, was also found to have activity against MBLs that was synergistic with the activity of MEM when they were used in combination (14).

The results also showed that serum had no substantial effect on the MICs of the TACN-MEM combination. The minimal or no effects of serum on the activity of MEM was attributed to MEM's low protein-binding properties (23). An investigation of the effects of serum on TACN or MEM MICs may allow speculation on the probable *in vivo* properties of the molecules at the preclinical stage. Furthermore, TACN did not affect the pharmacological properties of MEM, suggesting that TACN could have low plasma protein-binding properties either with or without MEM.

The MTT assay measures the ability of cells to reduce the MTT salt to a formazan product (24). This reaction can occur only in living cells with healthy mitochondria, as it is reliant on NADPH-dependent oxidoreductase enzymes. The cell viability obtained therefore reflects the number of viable cells present. TACN exposure resulted in a dose-dependent decrease in cellular metabolic activity and viability in HepG2 cells (Fig. 3). However, the IC_{50} obtained was ≥4-fold higher than the TACN inhibitory dose (8 mg/liter), and cell viability was 91% at the upper limit of the inhibitory dose. This analysis of the cytotoxicity of TACN showed that the compound possesses tolerable toxicity for the HepG2 cell line at the applied concentration and, hence, shows potential for development as an MBLI for clinical use.

An experimental assay, together with a computational simulation, demonstrated an excellent binding affinity between ligand and enzyme complexes as well as potential inhibitory properties. It is known that class B β-lactamases are susceptible to inhibition by chelating agents during interactions between the chelators (ligands) and the metal ions after ions are released from the protein (MBL) active site or while they are still associated with the enzyme complex (25). Overall, the calculated variation of the RMSD did not show considerable structural shifts, suggesting the stability of the enzyme structure and strength of ligand attachment inside the active-site pocket. The binding free energy analysis showed that the intermolecular van der Waals energy and the electrostatic interaction were the forces driving both systems. However, the total solvation energy (ΔG_{solv}) was unfavorable for all the complexes. Even though hydrogen bonds between the ligand and receptors were observed using LigPlot software and the Chimera molecular modeling tool (Fig. 7), their influences could not compensate for the substantial desolvation penalties during the interaction, thereby leading to the total solvation energy (ΔG_{solv}). Similar results where inhibition was dominated by the van der Waals interactions have been reported previously (26, 27).

In conclusion, this study showed that TACN inhibits class B1 MBL-producing CREs with a minimal cytotoxic effect at effective concentrations. TACN successfully potenti-

ated the antimicrobial properties of MEM and should thus be further investigated as an MBLI for clinical development in combination with carbapenems. Molecular modeling and docking studies demonstrated the mechanistic pathway by which TACN inhibits NDM-1 and VIM-2, sustaining a stable enzyme-ligand complex, with the caveat that this is only a simulation of a prediction and does not likely represent the actual binding mode. An in-depth analysis and optimization of the metal-chelating agent (TACN) employing a multidisciplinary research approach involving advanced computational simulations, biochemical and microbiological studies, and bioinformatics are needed in order to provide more evidence.

MATERIALS AND METHODS

Materials. Meropenem, TACN, dimethyl sulfoxide (DMSO), human serum, cation-adjusted Mueller-Hinton broth (CAMHB), Mueller-Hinton agar (MHA), phosphate-buffered saline (PBS), a β-lactamase inhibitor screening kit (MAK222), sterile-filtered serum from human male type AB plasma, and 3-(4,5-dimethyl-2-thiazolyl)-2,5-diphenyl-2H-tetrazolium bromide (MTT) were purchased from Sigma-Aldrich (St. Louis, MO, USA). Purified NDM-1 was obtained from RayBiotech, Norcross, GA, USA. Immortalized liver carcinoma (HepG2) cells and cell culture consumables were procured from Highveld Biologicals (Johannesburg, South Africa) and Whitehead Scientific (Johannesburg, South Africa), respectively.

Bacterial isolates. Seventeen carbapenem-resistant *Enterobacteriaceae* reference isolates (comprising 15 metallo-β-lactamase and 2 serine-β-lactamase producers), obtained from the Institut Pasteur (Paris, France) (Table 1) (28), and 33 clinical isolates producing metallo-β-lactamases, obtained from Lancet Laboratories (private sector, South Africa), were employed in this study (Table 2) (29). *Klebsiella pneumoniae* ATCC BAA 1706 and *Escherichia coli* ATCC 25922 were purchased from the American Type Culture Collection (ATCC) and were susceptible reference strains used for quality control. All bacterial isolates were fully characterized in previous studies for their phenotypic and genotypic resistance profiles (28, 29). The isolates were subcultured twice from freezer stocks onto MHA plates and incubated at 37°C before the experiments. All subsequent liquid subcultures were derived from colonies isolated from the agar plates and were grown in broth medium (CAMHB). Ethical approval for the used of clinical isolates was obtained from the Biomedical Research Ethics Committee of the University of KwaZulu-Natal, South Africa, under the reference number BE040/14.

Methods. (i) MICs and MBCs. MIC and minimum bactericidal concentration (MBC) determinations were performed according to Clinical and Laboratory Standards Institute (CSLI) guidelines (20) and the protocols described by Keepers et al. (30). Briefly, 2-fold dilutions of MEM and TACN ranging from 0.015 to 16 mg/liter and 1 to 64 mg/liter, respectively, were made with CAMHB in 96-well microtiter plates using the checkerboard method (14). A 0.5 McFarland-standardized bacterial inoculum was suspended into 200 μl CAMHB in each microtiter well. The plates were then incubated for 18 to 22 h at 37°C under aerobic conditions. The MIC was determined as the lowest concentration at which there was no visible growth. Afterwards, an aliquot of 100 μl was taken from the MIC assay wells in which no visible growth was observed and inoculated onto MHA plates for MBC determination by incubation at 37°C for 24 h. The MBC was determined to be the lowest concentration of the test compound that resulted in a viable bacterial count on the agar plates that was decreased $\geq$99.9% compared with the initial inoculum. Control wells were filled with the amount of solvent(s) used in dissolving the drug candidates, CAMHB, and bacteria. The experiments were conducted in triplicate.

(ii) Serum effects on MIC. The effects of serum on the MIC of the TACN-MEM combination were determined by a previously described method (31) and the above-mentioned MIC assay. In this assay, however, commercially available sterile-filtered serum from human male type AB plasma was added to the broth (CAMHB) to prepare 50% human serum in the final culture broth. Reference CRE strains carrying different enzymes (NDM-1, NDM-4, VIM-1, IMP-1, and IMP-8) were used to conduct this experiment.

(iii) Synergistic activity. A synergistic activity assay was used to describe the effect of the compounds (TACN and MEM) working together. The synergistic effect between TACN and MEM was determined by a previously described combination assay with a few modifications (32). Briefly, 2-fold serial dilutions of MEM were titrated with a fixed concentration (8 mg/liter) of TACN. This 8-mg/liter TACN concentration was the lowest concentration that did not inhibit the growth of bacteria alone but considerably potentiated the activity of MEM. MEM and TACN were also tested individually to determine their MICs. The fractional inhibitory concentration (FIC) index was calculated as follows: FIC of MEM [(MIC of MEM + TACN)/MIC of MEM alone] + FIC of TACN [(MIC of MEM + TACN)/MIC of TACN alone]. The effect/activity of a combination with an FIC index of $\leq$0.5 was considered synergistic, while an FIC index of 1 was defined as additive and an FIC index of $>$4 was characterized as antagonistic.

(iv) Time-kill assays. Time-kill assays were used to measure the quantitative kinetic kill model of TACN for the selected organisms and at different time points. Time-kill kinetic studies were conducted by previously reported methods (30), including those described by CLSI (20). *E. coli* carrying bla_{NDM-1}, *E. coli* carrying bla_{VIM-1}, as well as *E. cloacae* carrying bla_{IMP-1} were selected for use in this assay. Briefly, freshly prepared colonies were resuspended in 10 ml CAMHB and incubated in an orbital shaking incubator (37°C, 180 rpm) for 1 to 2 h. Cultures were then adjusted to a 0.5 McFarland standard (approximately 1.5×10^8 CFU/ml) and further diluted 1:20 in CAMHB so that the starting inoculum was approximately 1.5×10^6 CFU/ml. MEM was added to the prepared bacterial suspensions at final concentrations corresponding to 1×, 4×, or 8× the MIC of MEM while in combination with TACN at a fixed

concentration of 8 mg/liter. Also, the time-kill kinetics of 4× and 8× the MIC of MEM without TACN were investigated. A growth control with no antibiotic was included in the assay. The initial bacterial load was determined from the growth control test tube instantly after the dilution step and was recorded as the CFU count at time zero. The test tubes were incubated in an orbital shaking incubator at 37°C and 180 rpm, and bacterial cell viability counts were performed at 1, 2, 4, 6, 8, and 24 h by removing 100 μl of the culture, diluting it as appropriate, and plating it on MHA. The agar plates were incubated at 37°C for at least 22 h. The colonies were counted, and the results were recorded as the number of CFU per milliliter. A $\geq$3-$\log_{10}$ decrease in the number of CFU per milliliter within 24 h was considered bactericidal. The assays were executed in triplicate.

(v) Cytotoxicity assay. HepG2 cells were maintained at 37°C in 10% complete culture medium (CCM; Eagle's minimum essential medium supplemented with fetal bovine serum, antibiotics, and L-glutamine) until confluent. Following trypsinization, 1.5×10^4 cells/well were allowed to adhere to a 96-well plate overnight. The cells were treated with seven dilutions of TACN (16 to 1,024 mg/liter) prepared in CCM. Untreated cells (CCM only) served as the control. After 24 h, the treatment was replaced with 20 μl MTT solution (5 mg/ml MTT in PBS) and 100 μl CCM for 4 h. The resulting formazan product was solubilized in 100 μl DMSO (1 h), and the absorbance at 570 nm/690 nm was determined (BioTek μQuant plate reader; BioTek Instruments Inc., USA). The average absorbance values [(absorbance of treated cells/absorbance of control cells) × 100] were used to calculate cell viability and determine the IC_{50} (GraphPad Prism software, v7.05). All experiments were performed in triplicate.

(vi) Enzymatic assays: enzyme inhibition and inactivation kinetic parameters. The inhibitory effect of TACN was monitored by observing the rate of hydrolysis of the chromogenic compound nitrocefin, using purified preparations of a subclass B1 MBL enzyme (NDM-1) obtained from RayBiotech (Norcross, GA, USA). The assays were performed using a β-lactamase inhibitor screening kit (MAK222) according to the manufacturer's instructions. Briefly, 5 nM NDM-1 was preincubated with various concentrations of TACN varying from 0 to 50 μM at 25°C in a final experimental volume of 100 μl of β-lactamase assay buffer before adding nitrocefin. Nitrocefin hydrolysis was monitored at 25°C by following the variation of the absorbance at 490 nm using a plate reader spectrophotometer (SPECTROstar^{Nano}; BMG Labtech, Germany). The residual activity was determined and compared to that from the preincubation of the enzyme with the same procedure but without TACN. The effect of TACN-mediated inactivation of NDM-1 was determined by plotting the natural logarithm (ln)-linear plot of the percentage of the remaining enzyme residual activity versus the preincubation time, and the observed initial inactivation rate constant (K_{obs}) was calculated from the pseudo-first-order kinetic slope. The rate constant for enzyme inactivation (K_{inact}) and the inactivation constant (K_i) were calculated (GraphPad Prism software, v7.05; GraphPad Software Inc., San Diego, CA) according to the following hyperbolic equation previously described by Wong et al. (33): $K_{obs} = (K_{inact} - [I])/(K_i + [I])$, where K_{obs} is the observed initial inactivation rate constant for TACN inactivation and $[I]$ is the initial inhibitor concentration.

The preliminary mode of inhibition of NDM-1 by TACN was also assessed using the β-lactamase inhibitor screening kit reagents. Briefly, 500 nM purified NDM-1 was preincubated with 20 μM TACN at 25°C for 20 min, followed by rapid dilution with the addition of 30 μM nitrocefin, after which changes in the absorbance at 490 nm were monitored for 30 min. The experiments were conducted in triplicate.

Molecular modeling. For system preparation, the crystal structures (PDB accession numbers 5ZGE and 5ACU) were retrieved from the RSCB Protein Data Bank (https://www.rcsb.org/pdb/). The missing residues were added using a graphical user interface of Chimera, a molecular modeling tool (34). A ligand interaction map was generated using the web version of PoseView (35).

Molecular docking. Docking calculations were obtained using AutoDock Vina software (36). Geister partial charges were assigned, and the AutoDock atom types were defined using the AutoDock graphical user interface supplied by MGLTools (37). The docked conformations were generated using the Lamarckian genetic algorithm (LGA) (38). The binding affinities calculated for each of the two structures (enzyme-inhibitor complexes) were expressed in kilocalories per mole. This technique has been validated in previous studies (39). The grid box was defined using AutoDock Vina software, with the grid parameters being *x* equal to 26, *y* equal to 18, and *z* equal to 20 for the dimensions and *x* equal to −2.502, *y* equal to −5.255, and *z* equal to 32.723 for the center grid box. After using AutoDock Vina, the 10 conformations with the lowest binding energy were chosen for molecular docking.

Molecular dynamics simulation. Missing parameters for the ligand in the force field of Cornell et al. (40) were created in the absence of the available parameters. Optimization of the ligands was first performed at the HF/6-31G* level with the Gaussian 03 package. The restrained electrostatic potential (RESP) procedure (41) was used to calculate the partial atomic charges. General Amber force field (GAFF) (42) parameters and RESP partial charges were assigned using the Antechamber module in the Amber14 package. The hydrogen atoms of the proteins were added using the Leap module in Amber12. The standard Amber force field for bioorganic systems (ff03) was used to define the enzyme parameters. Counterions were added to neutralize the enzyme charge. The system was enveloped in a box of equilibrated TIP3P water molecules with an 8-Å distance around the enzyme. Cubic periodic boundary conditions were imposed, and the long-range electrostatic interactions were treated with the particle-mesh Ewald method (43) implemented in Amber12 with a nonbonding cutoff distance of 10 Å.

Initial energy minimization with a restraint potential of 2 kcal/mol Å^2 applied to the solute was carried out using the steepest-descent method in Amber12 for 1,000 iterations, followed by the conjugate gradient protocol for 2,000 steps. The entire system was then freely minimized for 1,000 iterations. Harmonic restraints with a force constant of 5 kcal/mol Å^2 were applied to all solute atoms during the heating phase. A canonical ensemble constant number (*N*), volume (*V*), and temperature (*T*) (*NVT*)

molecular dynamic (MD) simulation was carried out for 50 ps, during which time the system was gradually annealed from 0 to 300 K using a Langevin thermostat with a coupling coefficient of 1/ps. Subsequently, the system was equilibrated at 300 K with a 2-fs time step for 100 ps while maintaining the force constants on the restrained solute. The SHAKE algorithm (44) was employed on all atoms covalently bonded to a hydrogen atom during the equilibration and production runs. A production run was performed for 2 ns in an isothermal-isobaric (NPT) ensemble using a Berendsen barostat (45) with a target pressure of 1 bar and a pressure coupling constant of 2 ps with no restraints imposed. The coordinate file was saved every 1 ps, and the trajectory was analyzed every 1 ps using the Ptraj module implemented in Amber14.

ACKNOWLEDGMENTS

We are grateful to the South African National Research Foundation (grant no. 85595 awarded to S. Y. Essack as incentive funding for rated researchers) and the College of Health Sciences, University of Kwa-Zulu Natal, for funding this study. The College of Health Sciences, University of Kwa-Zulu Natal, Durban, South Africa, and the South African National Research Foundation (NRF) supported this study.

A.M.S., D.G.A., J.O.S., L.A.B., and S.Y.E. coconceptualized the study. A.M.S., D.G.A., H.M.K., and R.K. performed the experiments. A.M.S., D.G.A., H.M.K., and R.K. analyzed the data. All authors vetted the results. A.M.S. wrote the paper. All authors undertook critical revision of the manuscript.

We have no conflict of interest to declare.

REFERENCES

1. Wilke MS, Lovering AL, Strynadka NCJ. 2005. Beta-lactam antibiotic resistance: a current structural perspective. Curr Opin Microbiol 8:525–533. https://doi.org/10.1016/j.mib.2005.08.016.
2. Gaude G, Hattiholli J. 2013. Rising bacterial resistance to beta-lactam antibiotics: can there be solutions? J NTR Univ Health Sci 2:4–9. https://doi.org/10.4103/2277-8632.108504.
3. Heesemann J. 1993. Mechanisms of resistance to beta-lactam antibiotics. Infection 21:S4–S9. https://doi.org/10.1007/BF01710336.
4. Sekyere JO, Amoako DG. 2017. Carbonyl cyanide m-chlorophenylhydrazine (CCCP) reverses resistance to colistin, but not to carbapenems and tigecycline in multidrug-resistant Enterobacteriaceae. Front Microbiol 8:228. https://doi.org/10.3389/fmicb.2017.00228.
5. Hall BG, Salipante SJ, Barlow M. 2003. The metallo-β-lactamases fall into two distinct phylogenetic groups. J Mol Evol 57:249–254. https://doi.org/10.1007/s00239-003-2471-0.
6. Garau G, Garcia-Saez I, Bebrone C, Anne C, Mercuri P, Galleni M, Frere J-M, Dideberg O. 2004. Update of the standard numbering scheme for class B β-lactamases. Antimicrob Agents Chemother 48:2347–2349. https://doi.org/10.1128/AAC.48.7.2347-2349.2004.
7. Walsh TR, Toleman MA, Poirel L, Nordmann P. 2005. Metallo-β-lactamases: the quiet before the storm? Clin Microbiol Rev 18:306–325. https://doi.org/10.1128/CMR.18.2.306-325.2005.
8. Falconer SB, Reid-Yu SA, King AM, Gehrke SS, Wang W, Britten JF, Coombes BK, Wright GD, Brown ED. 2015. Zinc chelation by a small-molecule adjuvant potentiates meropenem activity in vivo against NDM-1-producing Klebsiella pneumoniae. ACS Infect Dis 1:533–543. https://doi.org/10.1021/acsinfecdis.5b00033.
9. Gupta N, Limbago BM, Patel JB, Kallen AJ. 2011. Carbapenem-resistant Enterobacteriaceae: epidemiology and prevention. Clin Infect Dis 53:60–67. https://doi.org/10.1093/cid/cir202.
10. Sekyere JO, Govinden U, Essack S. 2016. The molecular epidemiology and genetic environment of carbapenemases detected in Africa. Microb Drug Resist 22:59–68. https://doi.org/10.1089/mdr.2015.0053.
11. Osei Sekyere J. 2016. Current state of resistance to antibiotics of last-resort in South Africa: a review from a public health perspective. Front Public Health 4:209. https://doi.org/10.3389/fpubh.2016.00209.
12. World Health Organization. 2017. Global priority list of antibiotic-resistant bacteria to guide research, discovery, and development of new antibiotics. World Health Organization, Geneva, Switzerland.
13. Yoshizumi A, Ishii Y, Livermore DM, Woodford N, Kimura S, Saga T, Harada S, Yamaguchi K, Tateda K. 2013. Efficacies of calcium-EDTA in combination with imipenem in a murine model of sepsis caused by Escherichia coli with NDM-1 beta-lactamase. J Infect Chemother 19:992–995. https://doi.org/10.1007/s10156-012-0528-y.
14. King AM, Reid-Yu SA, Wang W, King DT, De Pascale G, Strynadka NC, Walsh TR, Coombes BK, Wright GD. 2014. Aspergillomarasmine A overcomes metallo-β-lactamase antibiotic resistance. Nature 510:503–506. https://doi.org/10.1038/nature13445.
15. Somboro AM, Sekyere JO, Amoako DG, Essack SY, Bester LA. 2018. Diversity and proliferation of metallo-β-lactamases: a clarion call for clinically effective metallo-β-lactamase inhibitors. Appl Environ Microbiol 84:e00698-18. https://doi.org/10.1128/AEM.00698-18.
16. Somboro AM, Tiwari D, Bester LA, Parboosing R, Chonco L, Kruger HG, Arvidsson PI, Govender T, Naicker T, Essack SY. 2015. NOTA: a potent metallo-β-lactamase inhibitor. J Antimicrob Chemother 70:1594–1596. https://doi.org/10.1093/jac/dku538.
17. McGeary RP, Tan DT, Schenk G. 2017. Progress toward inhibitors of metallo-β-lactamases. Future Med Chem 9:673–691. https://doi.org/10.4155/fmc-2017-0007.
18. Somboro AM, Amoako DG, Osei Sekyere J, Kumalo HM, Khan R, Bester LA, Essack S. 2019. Evaluation of 1,4,7-triazacyclononane (TACN) as a potential β-lactamase inhibitor in Enterobacteriaceae: restoring the activity of β-lactams. bioRxiv https://doi.org/10.1101/366146.
19. Weighardt P, Chaudhuri K. 1987. The chemistry of 1,4,7-triazacyclononane and related tridentate macrocyclic compounds. Prog Inorg Chem 35:329–436.
20. Clinical and Laboratory Standards Institute. 2017. Performance standards for antimicrobial susceptibility testing, 27th ed. Informational supplement M100-S27. Clinical and Laboratory Standards Institute, Wayne, PA.
21. Zhang Y, Hong H, Engle JW, Bean J, Yang Y, Leigh BR, Barnhart TE, Cai W. 2011. Positron emission tomography imaging of CD105 expression with a 64Cu-labeled monoclonal antibody: NOTA is superior to DOTA. PLoS One 6:e28005. https://doi.org/10.1371/journal.pone.0028005.
22. Azumah R, Dutta J, Somboro AM, Ramtahal M, Chonco L, Parboosing R, Bester LA, Kruger HG, Naicker T, Essack SY, Govender T. 2016. In vitro evaluation of metal chelators as potential metallo-β-lactamase inhibitors. J Appl Microbiol 120:860–867. https://doi.org/10.1111/jam.13085.
23. Craig WA, Welling PG. 1977. Protein binding of antimicrobials: clinical pharmacokinetic and therapeutic implications. Clin Pharmacokinet 2:252–268. https://doi.org/10.2165/00003088-197702040-00002.
24. Mosmann T. 1983. Rapid colorimetric assay for cellular growth and survival: application to proliferation and cytotoxicity assays. J Immunol Methods 65:55–63. https://doi.org/10.1016/0022-1759(83)90303-4.
25. Viswanatha T, Marrone L, Goodfellow V, Dmitrienko GI. 2008. Assays for beta-lactamase activity and inhibition. Methods Mol Med 142:239–260. https://doi.org/10.1007/978-1-59745-246-5_19.
26. Liang Z, Li L, Wang Y, Chen L, Kong X, Hong Y, Lan L, Zheng M, Guang-Yang C, Liu H, Shen X, Luo C, Li KK, Chen K, Jiang H. 2011.

Molecular basis of NDM-1, a new antibiotic resistance determinant. PLoS One 6:e23606. https://doi.org/10.1371/journal.pone.0023606.
27. Meini M-R, Llarrull L, Vila A. 2014. Evolution of metallo-β-lactamases: trends revealed by natural diversity and in vitro evolution. Antibiotics (Basel) 3:285–316. https://doi.org/10.3390/antibiotics3030285.
28. Nordmann P, Poirel L, Dortet L. 2012. Rapid detection of carbapenemase-producing Enterobacteriaceae. Emerg Infect Dis 18:1503–1507. https://doi.org/10.3201/eid1809.120355.
29. Osei Sekyere J, Amoako DG. 2017. Genomic and phenotypic characterisation of fluoroquinolone resistance mechanisms in Enterobacteriaceae in Durban, South Africa. PLoS One 12:e0178888. https://doi.org/10.1371/journal.pone.0178888.
30. Keepers TR, Gomez M, Celeri C, Nichols WW, Krause KM. 2014. Bactericidal activity, absence of serum effect, and time-kill kinetics of ceftazidime-avibactam against beta-lactamase-producing Enterobacteriaceae and Pseudomonas aeruginosa. Antimicrob Agents Chemother 58:5297–5305. https://doi.org/10.1128/AAC.02894-14.
31. Ramchuran EJ, Somboro AM, Abdel Monaim SAH, Amoako DG, Parboosing R, Kumalo HM, Agrawal N, De la Torre BG, Albericio F, Bester LA. 2018. In vitro antibacterial activity of Teixobactin derivatives on clinically relevant bacterial isolates. Front Microbiol 9:1535. https://doi.org/10.3389/fmicb.2018.01535.
32. Pankey GA, Ashcraft DS. 2005. In vitro synergy of ciprofloxacin and gatifloxacin against ciprofloxacin-resistant Pseudomonas aeruginosa. Antimicrob Agents Chemother 49:2959–2964. https://doi.org/10.1128/AAC.49.7.2959-2964.2005.
33. Wong SG, Fan PW, Subramanian R, Tonn GR, Henne KR, Johnson MG, Lohr MT, Wong BK. 2010. Bioactivation of a novel 2-methylindole-containing dual chemoattractant receptor-homologous molecule expressed on T-helper type-2 cells/D-prostanoid receptor antagonist leads to mechanism-based CYP3A inactivation: glutathione adduct characterization and prediction of in vivo drug-drug interaction. Drug Metab Dispos 38:841–850. https://doi.org/10.1124/dmd.109.031344.
34. Pettersen EF, Goddard TD, Huang CC, Couch GS, Greenblatt DM, Meng EC, Ferrin TE. 2004. UCSF Chimera—a visualization system for exploratory research and analysis. J Comput Chem 25:1605–1612. https://doi.org/10.1002/jcc.20084.
35. Stierand K, Rarey M. 2010. PoseView—molecular interaction patterns at a glance. J Cheminform 2(Suppl 1):P50. https://doi.org/10.1186/1758-2946-2-S1-P50.
36. Trott O, Olson AJ. 2010. Software news and update AutoDock Vina: improving the speed and accuracy of docking with a new scoring function, efficient optimization, and multithreading. J Comput Chem 31:455–461. https://doi.org/10.1002/jcc.21334.
37. Sanner MF. 1999. Python: a programming language for software integration and development. J Mol Graph Model 17:57–61.
38. Huey R, Morris GM, Olson AJ, Goodsell DS. 2007. A semiempirical free energy force field with charge-based desolvation. J Comput Chem 28:1145–1152. https://doi.org/10.1002/jcc.20634.
39. Kumalo HM, Soliman ME. 2016. Per-residue energy footprints-based pharmacophore modeling as an enhanced in silico approach in drug discovery: a case study on the identification of novel β-secretase1 (BACE1) inhibitors as anti-Alzheimer agents. Cel Mol Bioeng 9:175–189. https://doi.org/10.1007/s12195-015-0421-8.
40. Cornell WD, Cieplak P, Bayly CI, Gould IR, Merz KM, Ferguson DM, Spellmeyer DC, Fox T, Caldwell JW, Kollman PA. 1995. A second generation force field for the simulation of proteins, nucleic acids, and organic molecules. J Am Chem Soc 117:5179–5197. https://doi.org/10.1021/ja00124a002.
41. Cieplak P, Cornell WD, Bayly C, Kollman PA. 1995. Application of the multimolecule and multiconformational RESP methodology to biopolymers: charge derivation for DNA, RNA, and proteins. J Comput Chem 16:1357–1377. https://doi.org/10.1002/jcc.540161106.
42. Wang J, Wolf RM, Caldwell JW, Kollman PA, Case DA. 2004. Development and testing of a general Amber force field. J Comput Chem 25:1157–1174. https://doi.org/10.1002/jcc.20035.
43. Essmann U, Perera L, Berkowitz ML, Darden T, Lee H, Pedersen LG. 1995. A smooth particle mesh Ewald method. J Chem Phys 103:8577–8593. https://doi.org/10.1063/1.470117.
44. Ryckaert JP, Ciccotti G, Berendsen HJC. 1977. Numerical integration of the cartesian equations of motion of a system with constraints: molecular dynamics of n-alkanes. J Comput Phys 23:327–341. https://doi.org/10.1016/0021-9991(77)90098-5.
45. Berendsen HJC, Postma JPM, van Gunsteren WF, DiNola A, Haak JR. 1984. Molecular dynamics with coupling to an external bath. J Chem Phys 81:3684–3690. https://doi.org/10.1063/1.448118.